Bulletin of the Seismological Society of America, Vol. 102, No. 3, pp. 1030–1040, June 2012, doi: 10.1785/0120110255

Ⓔ

Evaluating Contributions to *SK*(*K*)*S* Splitting from Lower Mantle Anisotropy: A Case Study from Station DBIC, Côte D'Ivoire

by Colton Lynner and Maureen D. Long

Abstract Measurements of seismic anisotropy constitute a very important tool for examining patterns of flow and mineral properties in the Earth's mantle. A popular strategy for gaining insight into upper mantle processes is to examine the splitting of *SK(K)S* phases and interpret them in terms of upper mantle anisotropy and deformation; in such studies, any contribution to splitting from anisotropy in the lower mantle is usually ignored. Here we present measurements of *SKS* and *SKKS* splitting at Global Seismograph Network station DBIC in the Côte D'Ivoire, which exhibits a very unusual pattern of shear-wave splitting. The splitting pattern is dominated by null measurements over a wide range of back azimuths, with non-null measurements found over a very limited back-azimuthal range; we also identified examples of discrepant *SKS*–*SKKS* splitting for the same event–station pair. Splitting at DBIC has previously been interpreted in terms of upper mantle anisotropy, but we argue that this splitting pattern can best be explained by an apparently isotropic upper mantle with a contribution from anisotropy in the lower mantle, likely in the D″ layer. Using station DBIC as a case study, we discuss the potential pitfalls in interpreting *SKS*-splitting measurements and suggest a set of best practices to decrease the likelihood of misinterpreting shear-wave-splitting results at a seismic station.

Online Material: Summary of events used in the study, with their associated splitting parameters.

Introduction

Observations of seismic anisotropy yield some of the most direct constraints available to seismologists on patterns of mantle flow (e.g., Silver, 1996; Savage, 1999; Long and Becker, 2010). Anisotropy is usually understood to result from deformation; when an aggregate of an intrinsically anisotropic mineral (such as olivine) is subjected to deformation in the dislocation creep regime, it will develop a crystallographic or lattice preferred orientation (CPO or LPO) (e.g., Mainprice, 2007; Karato *et al.*, 2008). Observations of shear-wave splitting or birefringence, usually of core-refracted phases such as *SKS*, are a popular tool for studying mantle anisotropy; splitting is an unambiguous indicator of anisotropy, and codes that implement various shear-wave-splitting measurement algorithms are widely available.

From a ray theoretical point of view, shear-wave splitting is a path-integrated measurement, and the observed splitting will reflect contributions from anisotropy from anywhere along the ray path. For the core-refracted phases *SKS* and *SKKS*, splitting may therefore reflect anisotropy anywhere from the core–mantle boundary (CMB) to the surface on the receiver side of the ray path. In practice, however, *SK(K)S* splitting is nearly always interpreted in terms of anisotropy in the upper mantle beneath the receiver (e.g., Savage, 1999; Long and Silver, 2009; Long and Becker, 2010). This interpretation is based on inferences from mineral physics (e.g., Karato *et al.*, 1995, 2008) and comparisons of shear-wave-splitting measurements among body wave phases that have similar paths in the upper mantle but different paths in the lower mantle (e.g., Meade *et al.*, 1995; Niu and Perez, 2004).

Despite this first-order interpretation, however, several studies have presented evidence for local contributions to *SK(K)S* splitting from anisotropy in the lower mantle. Discrepancies between the splitting of *SKS* and *SKKS* phases for the same event–station pair were first documented by James and Assumpçao (1996) and have subsequently been documented in several regions, including at Global Seismographic Network (GSN) stations in Africa, Eurasia, and North America (Niu and Perez, 2004) and regional studies in Africa (Wang and Wen, 2007), South America (Vanacore and Niu, 2011), western North America (Long, 2009), and Japan (He and Long, 2011). Here we present *SK(K)S*-splitting measurements from DBIC, a long-running GSN station located in Côte d'Ivoire, western Africa. We find that DBIC exhibits a highly unusual splitting pattern, with null measurements observed at most back azimuths and a smaller number of non-null measurements mostly concentrated in one back-azimuthal swath. We also document two examples of *SKS–SKKS*-splitting discrepancies. Splitting measurements at DBIC have previously been interpreted in terms of upper mantle anisotropy (Barruol and Ben Ismail, 2001). Here we present an alternative hypothesis, which is that the upper mantle beneath DBIC is apparently isotropic (or is characterized by either a vertical axis of anisotropic symmetry or destructive interference of complex anisotropic layering that leaves shear waves unsplit) and that the non-null *SK(K)S*-splitting measurements reflect anisotropy in the lowermost mantle beneath Africa.

Data and Methods

Seismic station DBIC is located in the Côte d'Ivoire at 6.67° E, 4.86° S (Fig. 1) and has been in continuous service as part of the GSN since June 1994. We examined *SK(K)S* phases from over 700 earthquakes occurring between June 1994 and May 2011 using two simultaneous shear-wave splitting methods, the rotation-correlation method (e.g., Levin *et al.*, 1999) and the minimum energy method of Silver and Chan (1991). We selected events of magnitude $M_w \geq 5.8$ at epicentral distances between 90° and 130°. All waveforms were band-pass filtered to retain energy between 0.04 and 0.125 Hz; this filter is appropriate for retaining signal at the periods characteristic of *SK(K)S* phases (~10 s) while eliminating microseismic and cultural noise at periods shorter than 8 s. We visually inspected each waveform to insure good signal-to-noise ratios (SNRs; the noisiest arrival retained in the dataset had an SNR of the radial component of ~2, while the majority of the arrivals had SNRs > 3.5).

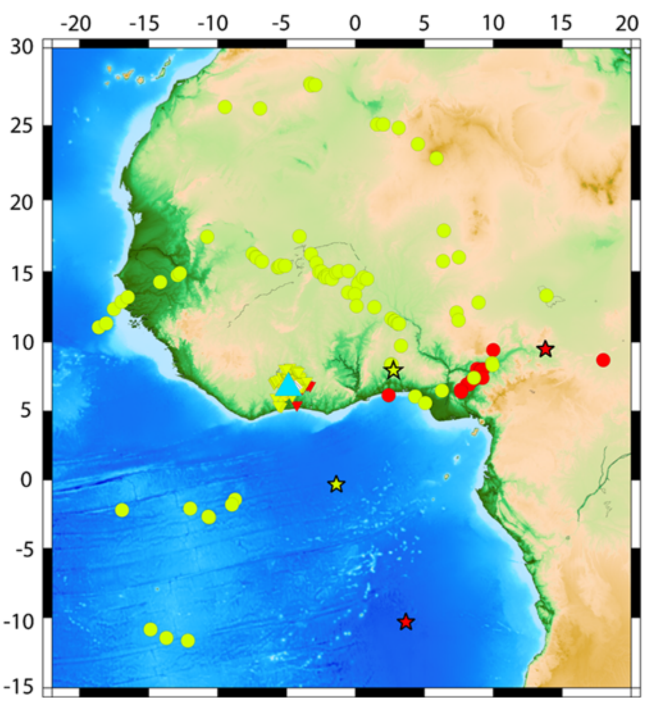

Figure 1. Map of the location of station DBIC (light-colored triangle), along with pierce points of *SKS* and *SKKS* phases in the shear-wave-splitting dataset plotted at a depth corresponding to the middle of the transition zone (510 km; inverted trianges) and a depth approximately corresponding to the top of the D″ layer (2700 km; circles). Null results are plotted in light colors, and split waves are plotted in dark colors. Stars designate discrepant *SKS–SKKS* pairs. The color version of this figure is available only in the electronic edition.

The simultaneous use of multiple splitting methods to measure the shear-wave-splitting parameters (fast direction ϕ and delay time δt) has been implemented by several studies (e.g., Vescey et al., 2008; Wirth and Long, 2008; Long and Silver, 2009; Huang *et al.*, 2011) and can help to ensure reliable results. We measured splitting using the Splitlab software package (Wüstefeld *et al.*, 2007). Windows were manually chosen to encompass at least one period of the signal. We rated each measurement as "good," "fair," or "poor," based on the quality of the data and of the results. Those we rated "good" had 2σ errors of less than $\pm 27°$ for ϕ and ± 1 s for δt. Consistency between the two splitting methods was also necessary for a "good" rating. The deviation between estimates of each splitting parameter calculated by the different methods was less than $\pm 9°$ and ± 0.1 s, respectively, for "good" results. "Fair" measurements had slightly larger errors, up to $\pm 35°$ for ϕ and ± 1.3 s for δt, and slightly larger differences between the two methods were allowed, up to $\pm 15°$ for ϕ and ± 0.6 s for δt. Null measurements were classified as such based on the linearity of the uncorrected particle motion for well-recorded *SKS* or *SKKS* arrivals and were given a quality rating based on the SNR and particle motion linearity. We only retained those measurements rated "fair" or "good" when we evaluated the overall pattern of shear-wave splitting at the station. Examples of typical null measurements are shown in Figure 2, and examples of typical non-null measurements are shown in Figure 3.

During our shear-wave-splitting analysis, we identified a misalignment of the horizontal components for station DBIC, based on polarization analysis of the *SK(K)S* phases. Because the polarization of *SK(K)S* phases is controlled by the *P*-to-*SV* conversion at the CMB, the incoming polarization should align with the back azimuth. We identified a systematic misalignment of the initial polarizations of $16° \pm 2°$ relative to the back azimuth, consistent with previous studies (e.g., Schulte-Pelkum *et al.*, 2001, who used *P*-polarization analysis to characterize the misalignment at DBIC). We found that the misalignment of ~16° persisted throughout the time period examined in this study (1994–2011), which rules out an intermittent sensor orientation problem. Uncorrected horizontal component misalignments can cause systematic errors in shear-wave-splitting analysis, including disagreement among different measurement methods (e.g., Tian *et al.*, 2011; Hanna and Long, 2012). We corrected for the measured misalignment by rotating all the horizontal records by +16° before measuring the splitting. We also routinely evaluated the initial polarization direction of the split *SKS* phases (after correction for horizontal component misalignments) in order to ensure that the initial polarizations were consistent

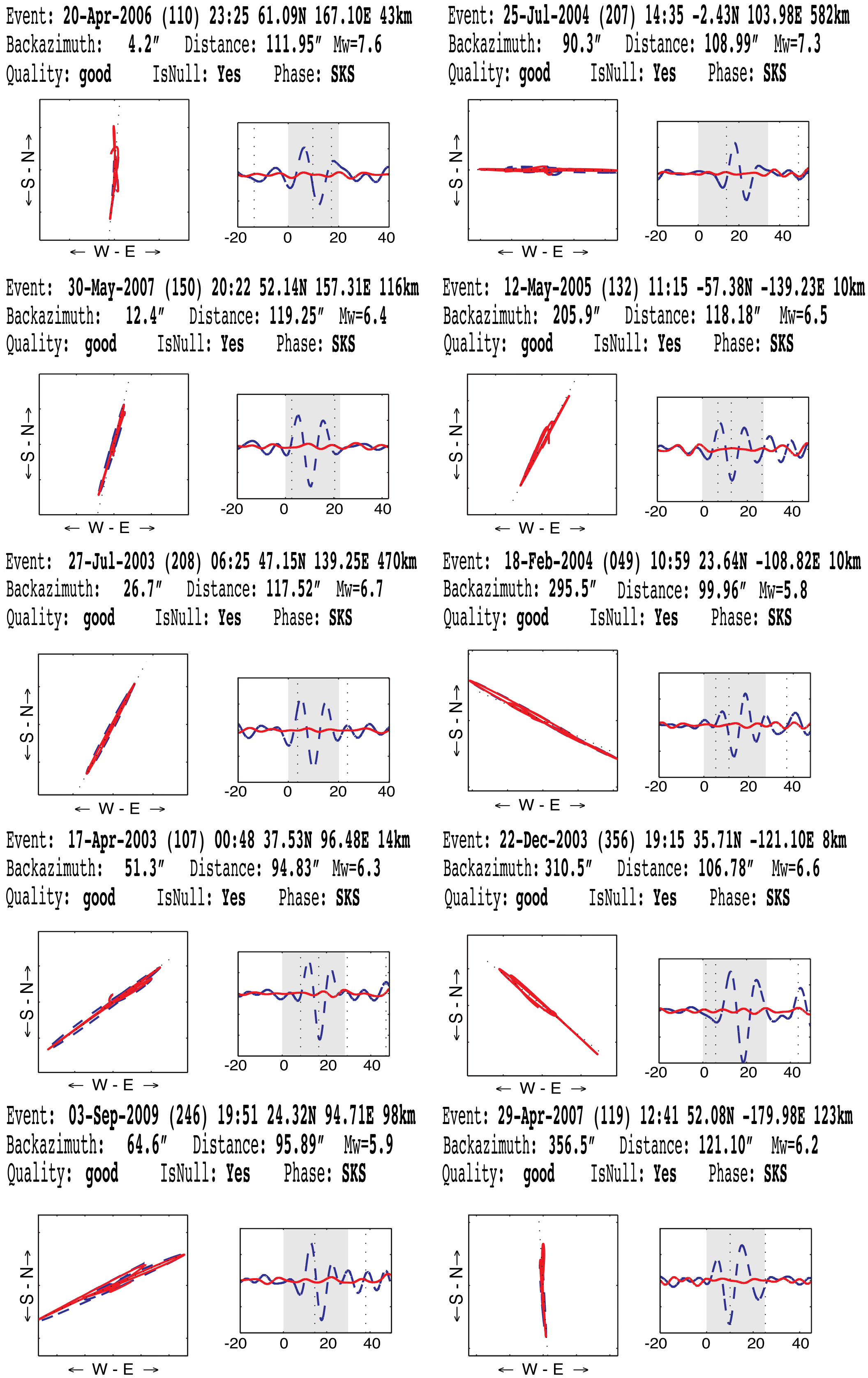

Figure 2. Examples of null measurements from various back azimuths. For each arrival, the left plot shows the uncorrected particle motions. The right plot shows the uncorrected radial (dashed) and transverse (solid) waveforms. The color version of this figure is available only in the electronic edition.

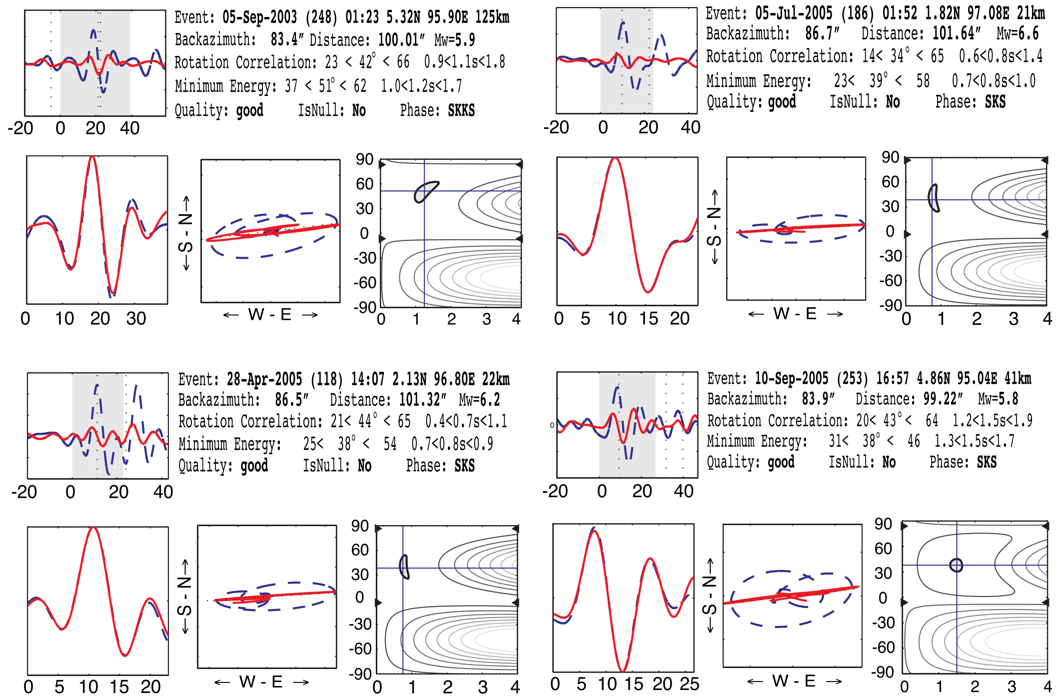

Figure 3. Four examples of non-null splitting measurements. For each arrival, four diagnostic plots are shown. The uncorrected radial (dashed) and transverse (solid) waveforms are shown at top left. Diagnostic plots for the transverse component minimization method are shown in the bottom row (left to right): the corrected fast (dashed) and slow (solid) shear waveforms; the uncorrected (dashed) and corrected (solid) particle motion diagrams; and the energy map of the transverse component, with the 95% confidence region shown as a gray ellipse and the best-fitting splitting parameters shown with a cross. The color version of this figure is available only in the electronic edition.

with the expected polarization for a *P*-to-*SV* conversion at the CMB (that is, that the initial polarizations were aligned with the back azimuth). *SK(K)S* polarizations can be affected by heterogeneous Earth structure (e.g., Restivo and Helffrich, 2006); and, in cases in which the initial polarizations are not aligned with the back azimuth, energy may be present on the transverse component that is not due to anisotropy. For all *SK(K)S*-splitting measurements retained in our dataset, the measured initial polarizations were aligned with the back azimuth (within the error on the initial polarization measurement, estimated to be about 10°).

Results

Our measurement procedure yielded 80 null and 23 non-null results for *SSK* and *SKKS* phases. The splitting dataset is shown in stereo plot form in Figure 4, in which the null and non-null measurements are plotted as a function of back azimuth and incidence angle, and in table form in Ⓔ Table S1 of the electronic supplement to this paper. The back-azimuthal coverage of the earthquakes recorded at station DBIC is quite good. We identified well-recorded null results across most back azimuths (Fig. 4), with nulls recorded in all four back-azimuthal quadrants and the entire back-azimuthal swath from approximately −70° to 70°, which is densely populated with nulls. We did, however, identify a population of 22 non-null splits occupying a narrow back-azimuthal

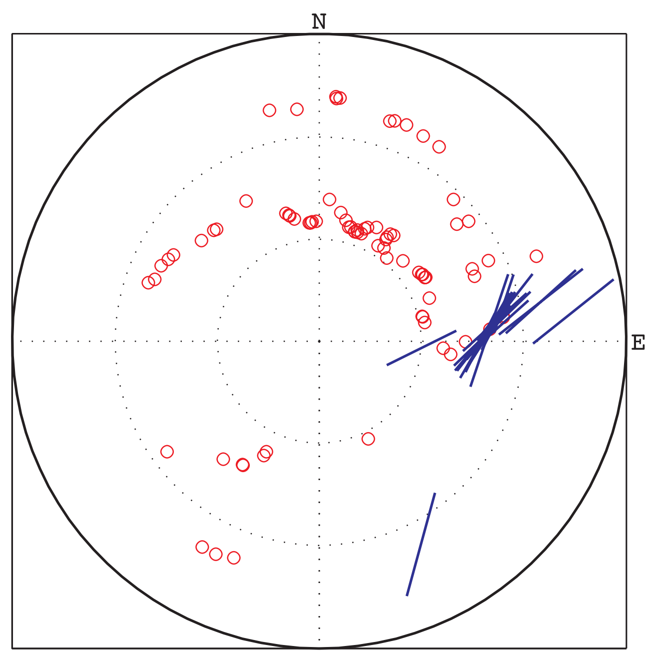

Figure 4. A stereographic plot of null (circles) and non-null (bars) *SKS* and *SKKS* splitting measurements, plotted as a function of back azimuth (angle from the north) and incidence angle (distance from origin). The color version of this figure is available only in the electronic edition.

swath around ~90° and a single non-null result coming from a back azimuth of ~155°. Most splits (18 results) are recordings of *SKS* phases, but we also observed three split *SKKS* phases. The non-null measurements coming from the ~90° back azimuth exhibit very consistent ϕ and δt (Fig. 4), with an average fast direction of ~36° and an average delay time of ~1 s. All the non-null measurements shown in Figure 4 were rated as "good" or "fair" and are well constrained (Fig. 3). While a few null measurements are present in the ~90° back-azimuthal non-null swath (Fig. 1), the region is heavily dominated by split measurements.

We also recorded two instances of a single earthquake yielding discrepant shear-wave splitting between *SKS* and *SKKS* phases (shown in Figs. 5 and 6). In both instances, the *SKS* phase yielded a null result, while the corresponding *SKKS* arrival was significantly split. One of the discrepant *SKS–SKKS* pairs recorded shear-wave-splitting parameters similar to those seen for the rest of the measurements near ~90° back azimuth. The other *SKS–SKKS* pair arrived from a back azimuth of ~155° and represents the only measurements that sample the mantle at that geometry (Figs. 1 and 4).

Discussion

The pattern of splitting seen at station DBIC is quite striking, with null measurements dominating at most back azimuths but with a group of consistent non-null measurements at a back azimuth of ~90° and one non-null at ~155° (Fig. 4). What kind of anisotropic structure in the mantle could cause this unusual splitting pattern? For the simple case of a single, horizontal, laterally homogeneous layer of anisotropy in the upper mantle, we would expect to observe a simple splitting pattern, with consistent splitting parameters recorded at most back azimuths and null results at back azimuths corresponding to the directions of fast and slow wave propagation. In the case of isotropy or hexagonal anisotropy with a vertical axis of symmetry, we would expect to observe null splitting over all back azimuths. The splitting pattern we observe at station DBIC is not consistent with either of these simple cases. This leads to the conclusion that the anisotropy is more complicated than the simplest upper mantle anisotropy scenarios. The observation of back-azimuthal complexity in the splitting pattern suggests either lateral or vertical heterogeneity in anisotropic structure. Multiple layers of anisotropy would be expected to produce back-azimuthal variations in shear-wave splitting, but we would expect a 90° periodicity in apparent splitting parameters with back azimuth for vertically stratified anisotropy (e.g., Silver and Savage, 1994). This suggests that lateral heterogeneity in anisotropic structure somewhere in the mantle sampled by the *SK(K)S* phases is required to explain the splitting observations at DBIC.

Insight into the nature and location of this lateral anisotropic heterogeneity can be gained by considering how the *SK(K)S* phases recorded at DBIC sample different regions of the mantle. Figure 1 shows the pierce points of the *SKS* and *SKKS* phases for which splitting was measured (either null or non-null) at depths of 510 km (in the middle of the transition zone) and at 2700 km (at the top of the D″ layer at the base of the mantle). We also considered the location of pierce points at a depth of 200 km, which corresponds to the mid-upper mantle, but they would plot under the symbol marking the station location in Figure 1. The group of split *SK(K)S* phases from ~90° back azimuth sample the transition zone and upper mantle at locations that are very close to the pierce points for the null *SK(K)S* phases, with lateral separations of less than ~50 km. Dramatic heterogeneity on such short-length scales in the asthenospheric upper mantle or transition zone seems unlikely; and, even if such heterogeneity were present, the first Fresnel zones (zones of highest finite-frequency sensitivity) for *SK(K)S* phases with periods of ~10 s are on the order of ~100 km wide (e.g., Favier and Chevrot, 2003), and it would be difficult to obtain the highly variable splitting pattern shown in Figure 4.

We also consider whether the DBIC splitting pattern could be produced by small-scale heterogeneity in anisotropic structure in the crust (or shallow mantle lithosphere), but that seems an unlikely explanation as well. Lateral heterogeneity of less than ~10 km in crustal structure would be required to produce the observed splitting; and, because typical delay times due to crustal anisotropy are ~0.1 s (e.g., Kaneshima, 1990; Long and Silver, 2009), this is not a likely explanation for the ~1 s of *SK(K)S* splitting observed at back azimuths near ~90° at DBIC. A few recent studies have argued that crustal anisotropy may have a larger effect on the splitting of *SK(K)S* phases than the ~0.1 s that is typically assumed; for example, Kaviani *et al.* (2011) argue for strong crustal influence on shear-wave-splitting parameters in the Dead Sea basin, and Mattatall and Fouch (2007) documented a strong influence on *SKS* splitting from crustal anisotropy near Parkfield, California. However, the abrupt transition in splitting behavior we observe at DBIC from null splitting to delay times of over 1 s is sharper than the transitions attributed to crustal anisotropy by these authors. While an influence from crustal anisotropy cannot be entirely ruled out at DBIC, we do not consider it to be a likely explanation for the unusual *SK(K)S*-splitting pattern documented here.

We argue that the most likely explanation for the splitting pattern shown in Figure 4 is an apparently isotropic upper mantle beneath the station, with a localized region of coherent anisotropy at the base of the mantle in the D″ layer to the east of the station and some lowermost mantle anisotropy to the south as well. D″ has been shown to be strongly anisotropic in many regions (e.g., Karato, 1998; Kendall and Silver, 1998; Garnero *et al.*, 2004; Wookey and Kendall, 2007; Nowacki *et al.*, 2011). The presence of anisotropy in D″ is in contrast to the bulk of the overlying lower mantle, which is generally thought to be isotropic (e.g., Meade *et al.*, 1995) as it is deforming via a diffusion creep mechanism that does not produce LPO (e.g., Karato *et al.*, 1995). When we plot the pierce points of the *SK(K)S* phases at a depth associated with the D″ layer (Fig. 1), we see that the region

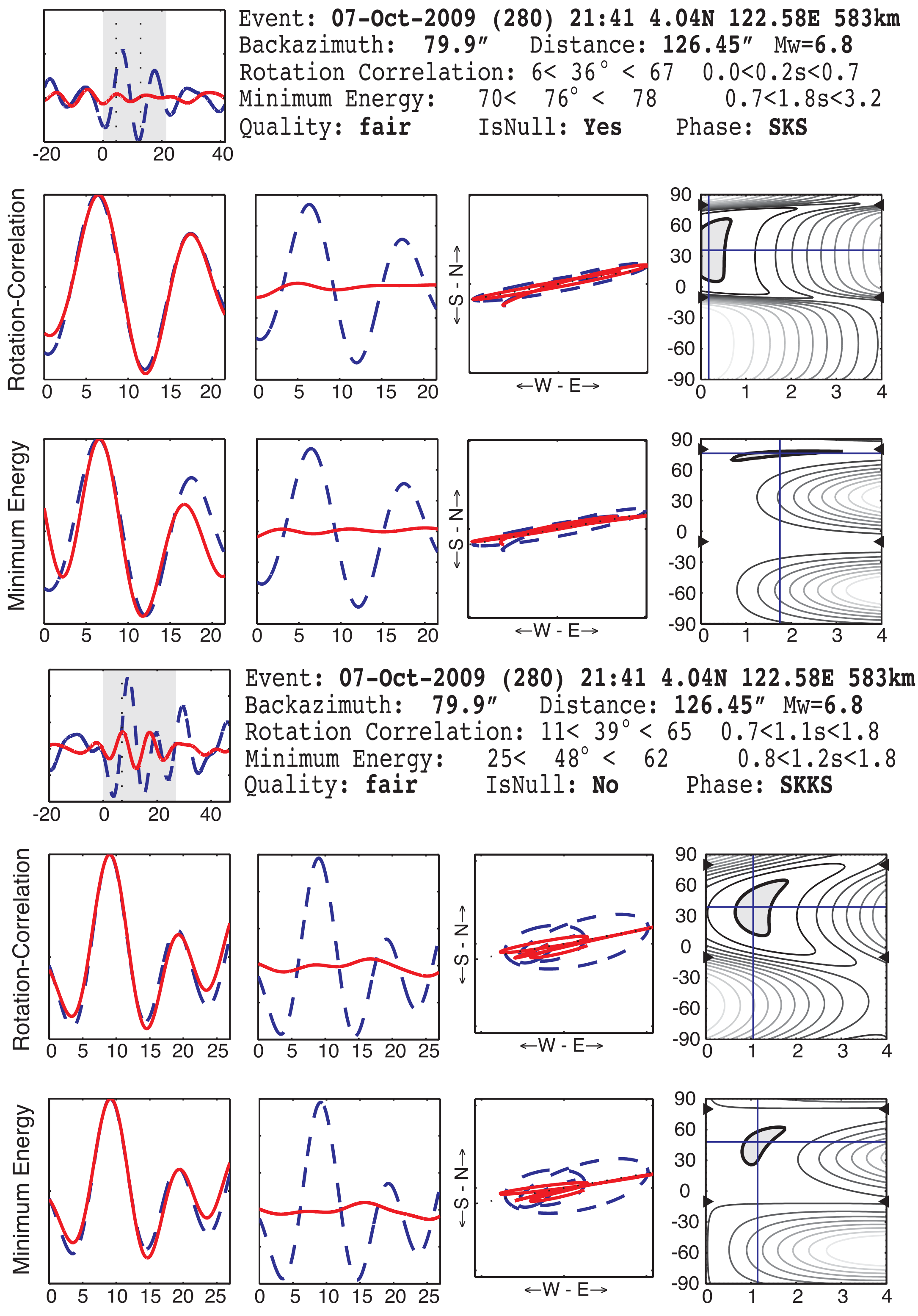

Figure 5. Waveforms and splitting diagnostic plots for an event on 7 October 2009, which yielded discrepant *SKS* and *SKKS* splitting for the same event–station pair. The top set of plots corresponds to the *SKS* phase, while the bottom set corresponds to the *SKKS* phase. At top left of each set, the uncorrected radial waveforems as shown as dashed lines, and the transverse waveforms are shown as solid lines. The middle row of each set shows diagnostic plots for the rotation-correlation method (left to right): the corrected fast (dashed) and slow (solid) shear waveforms; the corrected radial (dashed) and transverse (solid) waveforms; the uncorrected (dashed) and corrected particle motion diagrams; and the energy map of the transverse component, with the 95% confidence region shown as a gray ellipse and the best-fitting splitting parameters shown with a cross. The bottom row of each set shows the same diagnostic plots for the transverse component minimization method. The color version of this figure is available only in the electronic edition.

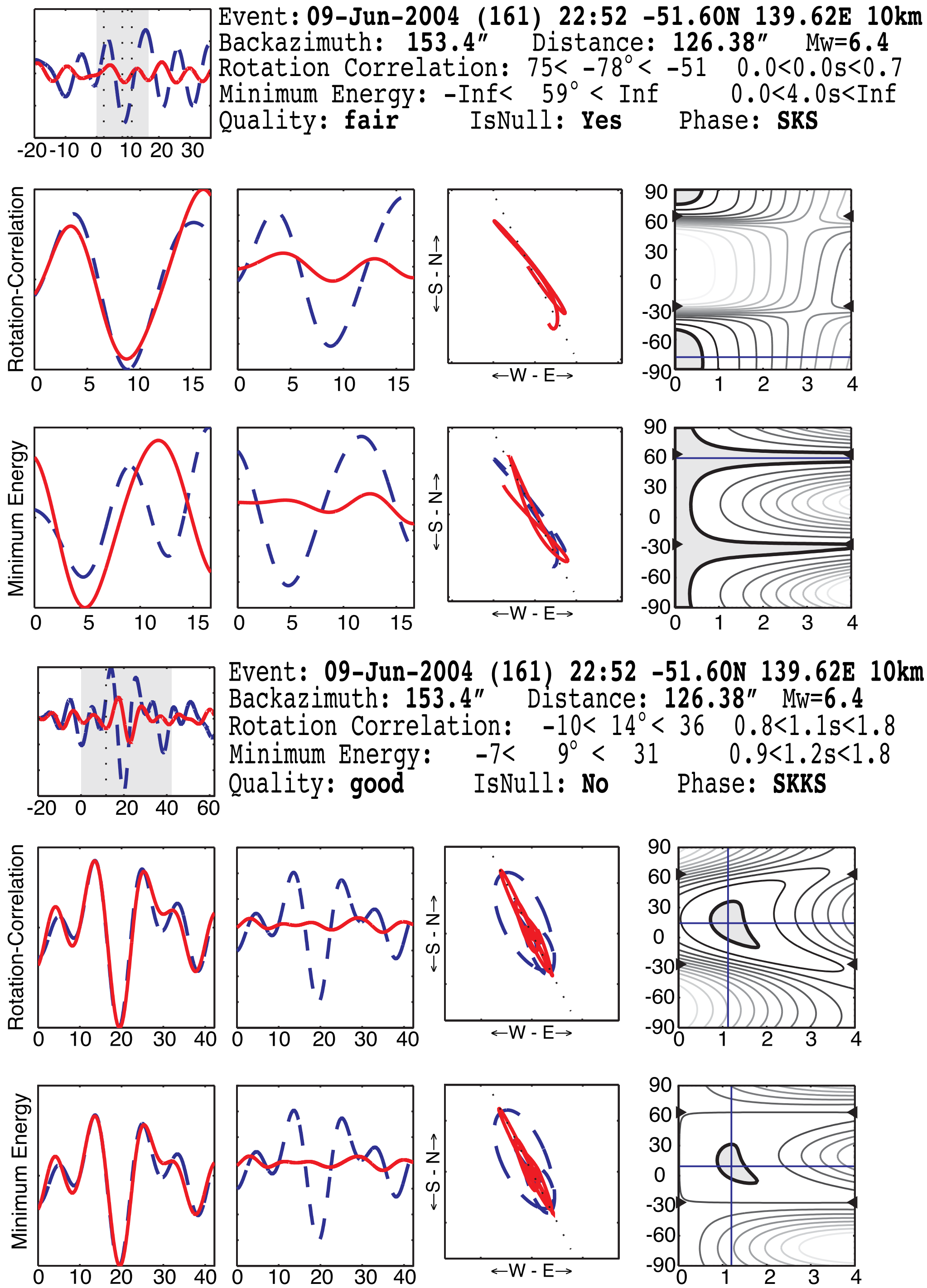

Figure 6. Waveforms and splitting diagnostic plots for an event on 9 June 2004, which yielded discrepant *SKS* and *SKKS* splitting for the same event–station pair. Plotting conventions are as in Figure 5. The color version of this figure is available only in the electronic edition.

sampled by split *SK(K)S* waves and the closest region sampled by null *SK(K)S* arrivals are separated by ~350 km at a depth of 2700 km, a reasonable length scale for heterogeneity in anisotropic structure. As noted previously and as shown in Figure 1, the region sampled by the split *SK(K)S* arrivals is also sampled by three *SKS* arrivals that are not split. There is no immediately obvious explanation for this observation, but we note that other studies that have found evidence for lowermost mantle contributions to *SK(K)S* splitting have identified similar patterns of a few null measurements interspersed with measurements that show significant splitting (e.g., Long, 2009; He and Long, 2011).

The two examples of discrepant splitting between *SKS* and *SKKS* for the same event observed at DBIC support the argument for a primary influence of D″ anisotropy on the observed splitting. Previous studies have examined anisotropy at the base of the mantle using discrepant *SKS*–*SKKS* splitting (e.g., Niu and Perez, 2004; Restivo and Helffrich, 2006; Wang and Wen, 2007; Long, 2009; He and Long, 2011). These studies have argued that the ray paths of *SKS* and *SKKS* are too similar in the upper mantle to attribute the observed discrepancies to upper mantle anisotropy, and placing the anisotropy in the transition zone would require unreasonably small-scale anisotropic heterogeneities (less than ∼70 km) compared to the Fresnel zones of the waves under study (e.g., Long, 2009). In contrast, the pierce points in D″ for *SKS* and *SKKS* at epicentral distances between ∼110° and 120° are ∼750 km apart, so the two phases sample different regions of the lowermost mantle. The two examples of discrepant *SKS*–*SKKS* splitting in our DBIC dataset involve null *SKS* arrivals with corresponding *SKKS* delay times of ∼1 s; this requires a change in anisotropic structure over length scales of several hundreds of kilometers at the base of the mantle. The *SKS*–*SKKS* discrepancies we observe provide another line of evidence that the *SK(K)S* splitting observed at DBIC is due to anisotropy in the D″ region rather than in the upper mantle. This inferred mechanism differs from previous interpretations of *SK(K)S* splitting at DBIC, which has been attributed to anisotropy and flow in the upper mantle (Barruol and Ben Ismail, 2001).

Further support for the idea that the upper mantle beneath DBIC is apparently isotropic and the observed *SK(K)S* splitting is due mainly to D″ anisotropy comes from previous work to characterize D″ anisotropy beneath Africa. Discrepancies between *SKS* and *SKKS* have been documented at several African seismic stations in addition to DBIC; GSN seismic station BGCA in Africa exhibits discrepant *SKS*–*SKKS* splitting (Niu and Perez, 2004), and Wang and Wen (2007) used several other African stations to probe anisotropy at the base of the mantle with *SK(K)S* phases. Specifically, Wang and Wen (2007) documented *SKS*–*SKKS*-splitting discrepancies for phases that sample the lowermost mantle beneath Africa and found that the inferred anisotropic structure generally coincides geographically with edges of the very low velocity province (VLVP) beneath Africa (Fig. 7). The African VLVP is located just above the core–mantle boundary, and Wang and Wen (2007) argued that the observed discrepancies in *SK(K)S* splitting arise from the complex anisotropy due to mantle flow at the margin of the VLVP. The eastern boundary of the VLVP was well sampled by the Wang and Wen (2007) study, and its location is thus well constrained, with many *SKS*–*SKKS* discrepancies observed for waves that sample D″ along the boundary (red-shaded region in Fig. 7). In contrast, Wang and Wen (2007) found that most splitting parameters for *SKS* and *SKKS* phases were very similar for waves that sampled D″ beneath the center of the continent and the center of the VLVP (dark-blue-shaded region in Fig. 7). Even in this region of consistent *SKS*–*SKKS* splitting, however, Wang and Wen (2007) did identify a few

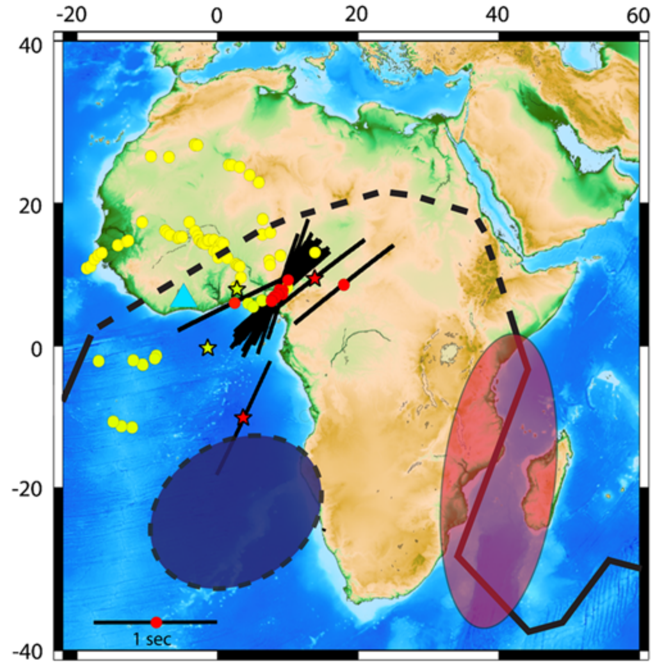

Figure 7. Pierce points of *SKS* and *SKKS* phases at a depth of 2700 km, corresponding to the top of the D″ layer. Station DBIC is shown with a large triangle. Pierce points for null measurements are plotted as light-colored circles; pierce points for non-null measurements are plotted as dark-colored circles. Discrepant *SKS*–*SKKS* pairs are plotted with stars. The shear-wave-splitting parameters (ϕ, δt) for the non-null measurements are plotted as black bars at the pierce point, with the orientation and length of the bar corresponding to the fast-splitting direction and the delay time, respectively. The thick black line corresponds to the edge of the lower mantle very low velocity province (VLVP) beneath Africa, as inferred by Wang and Wen (2007). The location of its northern boundary, shown with a dashed line, was not well constrained by their study. The solid shaded region indicates where Wang and Wen (2007) inferred anisotropy in the lowermost mantle from *SKS*–*SKKS* splitting discrepancies. The dashed shaded region indicates where Wang and Wen (2007) found only a few examples of a contribution to *SK(K)S* splitting from lowermost mantle anisotropy. The color version of this figure is available only in the electronic edition.

examples of contributions to *SK(K)S* splitting from lower mantle anisotropy in this region at the center of the VLVP.

While the anomalous anisotropy associated with the eastern border of the VLVP was well defined in the Wang and Wen (2007) study, their dataset lacked the necessary coverage to sample its northern border. If the model put forward by Wang and Wen (2007) is correct and the anomalous anisotropy beneath Africa that results in *SKS*–*SKKS* discrepancies is associated with the edge of the VLVP, then we hypothesize that the region of locally unusual D″ anisotropy sampled by *SK(K)S* waves to the east of DBIC may correspond to the northern border of the African VLVP (dashed line, Fig. 7). (While one of the *SKS*–*SKKS* discrepancies that we observed samples the lowermost mantle to the south of DBIC and does not sample the inferred northern border, it is consistent with the finding of Wang and Wen (2007) that a small minority of

SK(K)S phases that sample this region do exhibit splitting due to lowermost mantle anisotropy.) Our inference of a coherent region of lowermost mantle anisotropy to the east of DBIC that is sampled by *SK(K)S* phases arriving from the east thus helps to constrain the northern edge of the VLVP and further supports the notion of lowermost mantle anisotropy beneath Africa (Wang and Wen, 2007).

Our hypothesis that the non-null *SK(K)S* splitting observed at DBIC is due to anisotropic structure in the lower mantle requires that the upper mantle beneath the station is apparently isotropic, as discussed previously in this paper. There are several potential explanations for this, although our observations cannot discriminate among the different possibilities. One explanation is that the upper mantle beneath the station is actually isotropic or only weakly anisotropic, perhaps due to negligible recent strain accumulation in the asthenosphere. Some recent global models of mantle flow that include both plate- and density-driven flow (e.g., Becker, 2008; Conrad and Behn, 2010) do predict substantially weaker flow in the asthenospheric upper mantle beneath western Africa compared to other regions and might be consistent with this scenario. Another possibility is that the upper mantle has a vertical fast axis of hexagonal or nearly hexagonal anisotropic symmetry, which might be consistent with localized vertical flow beneath the station (perhaps associated with small-scale convection). A third possibility is that there is anisotropic layering in the upper mantle that results in destructive interference of splitting; for example, if there are two layers with equal anisotropic strength for which the fast directions are offset by exactly 90°, then vertically propagating *SKS* waves would not be significantly split.

Implications for *SKS*-Splitting Studies

Shear-wave splitting is perhaps the most popular technique for probing the anisotropic structure and dynamics of the upper mantle, and the splitting of *SK(K)S* phases is nearly always interpreted as being due to upper mantle anisotropy. There are several lines of evidence to suggest that, to first order, this interpretation is usually correct. The upper mantle is likely deforming via dislocation creep, which produces olivine LPO and macroscopic seismic anisotropy (e.g., Karato *et al.*, 2008), while the lower mantle, with the possible exception of D″, is thought to be in the diffusion creep regime (e.g., Karato *et al.*, 1995). From an observational point of view, global comparisons among *SKS*-splitting measurements and models for upper mantle anisotropy derived from surface waves (which are not sensitive to lowermost mantle structure) are, to first order, successful (e.g., Wüstefeld *et al.*, 2009; Becker *et al.*, 2012), indicating that upper mantle anisotropy is the primary contribution to *SK(K)S*-splitting datasets globally. Global studies of *SKS*–*SKKS*-splitting discrepancies indicate that in 95% of cases, there is no indication of a contribution to SK(K)S splitting from the lowermost mantle (Niu and Perez, 2004; Restivo and Helffrich, 2006).

Seismic anisotropy in the deepest mantle does not make a primary contribution to the global *SK(K)S*-splitting dataset, but there is increasing evidence for geographically localized contributions to the splitting of *SK(K)S* phases from anisotropy in the lowermost mantle, including the splitting patterns at station DBIC documented in this study. It is important for shear-wave-splitting practitioners to be aware of this possibility for two reasons. The first is that constraints on seismic anisotropy in D″ can yield insights into geodynamic processes and perhaps flow patterns at the base of the mantle. Because of the nonuniform coverage of earthquakes and seismic stations at the Earth's mantle, only a few regions of D″ have been investigated for anisotropic structure, and *SK(K)S* phases may sample different regions of lowermost mantle than other phases commonly used to probe D″ anisotropy. The second reason, more germane to studies of the upper mantle, is that any contribution to *SK(K)S* splitting from lowermost mantle anisotropy may contaminate the upper mantle anisotropy signal. If splitting due to D″ anisotropy is erroneously attributed to the upper mantle, it will lead to misinterpretation of upper mantle structure and dynamics.

In order to ensure that any contribution to *SK(K)S* splitting from the lowermost mantle is identified, evaluated, and (in studies of upper mantle anisotropy) accounted for, we suggest a set of best practices in *SK(K)S*-splitting studies. First, it is important to obtain the best back-azimuthal coverage possible. It is well known that good back-azimuthal coverage is needed to properly evaluate the possibility of multiple layers of upper mantle anisotropy beneath a seismic station (e.g., Silver and Savage, 1994); such good coverage is also useful when trying to evaluate any contribution from lowermost mantle anisotropy. Obtaining sufficient back-azimuthal coverage is often difficult, due to the highly nonuniform distribution of global seismicity, and this is a major (and well-known) limitation in *SK(K)S*-splitting studies. In order to increase the back-azimuthal coverage, it is prudent to examine all available data for permanent or long-running stations and, when practical, to increase deployment durations for temporary stations. The back-azimuthal coverage can also sometimes be improved by using other phases, such as *PKS* or *S3KS*. It is possible to greatly improve the back-azimuthal coverage beneath a seismic station by including measurements of the splitting of direct teleseismic *S* phases (e.g., Long and van der Hilst, 2005), but this introduces an additional source of potential error, as there may be a contribution to splitting from anisotropy near the source.

A second important aspect of shear-wave-splitting studies that can help to shed light on any contribution from the lowermost mantle is the careful measurement and interpretation of null (that is, nonsplit) *SK(K)S* arrivals. Null *SK(K)S* splitting can be attributed to isotropic mantle on the receiver side, to the destructive interference of multiple layers or regions of anisotropy, or to the alignment of the initial polarization of the wave with a fast or slow symmetry axis of the anisotropic medium. Observations of null *SK(K)S* splitting are common even for the simplest case of a single, horizontal layer of anisotropy at depth, and they are sometimes overlooked in splitting datasets. At station DBIC, the pattern of null splitting over a wide range of back azimuths is crucial to determining the most likely source of anisotropy, as argued previously in this paper. It is critical to measure the back-azimuthal distribution of null measurements in *SK(K)S*-splitting datasets in order to determine whether they are consistent with a simple anisotropic model (such as a single horizontal layer) or whether vertical and/or lateral variations in anisotropic structure are required by the data.

A third best practice in the analysis of shear-wave-splitting datasets is the routine identification and analysis of *SKS–SKKS* splitting discrepancies for the same event–station pairs. Because strongly discrepant *SKS–SKKS* splitting can be reliably attributed to anisotropy in the lower mantle on the receiver side, observations of discrepancies provide a red flag that all *SK(K)S* splitting should not be attributed to upper mantle anisotropy at a given station. It is therefore important to routinely identify and compare pairs of *SKS* and *SKKS* phases for which splitting (or lack of splitting) can be constrained. This can be difficult, particularly for temporary stations with short deployment times, as there is a limited epicentral distance range at which *SKS* and *SKKS* phases both have high amplitudes (~110°–120°). Nevertheless, *SKS–SKKS* discrepancies should be routinely considered in shear-wave-splitting studies; when present, they provide a clue to anomalous anisotropic structure in D″, while their absence can give confidence to shear-wave-splitting analysts that *SK(K)S* splitting measurements mainly reflect anisotropy in the upper mantle.

Summary

We have evaluated the pattern of *SK(K)S* splitting at station DBIC in detail and find that the splitting pattern is dominated by nulls at most back azimuths, with a group of well-constrained non-null splitting measurements at a back azimuth of ~90° and a single non-null measurement at ~155°. *SK(K)S* splitting at DBIC has been interpreted as being due to upper mantle anisotropy beneath the station in the past (e.g., Barruol and Ben Ismail, 2001), but here we propose an alternative model to explain the data. We argue that the overall pattern of splitting, and the observation of discrepant *SKS–SKKS* splitting, is best explained by anisotropy in the D″ region at the base of the mantle. Our interpretation supports previous work that has suggested the presence of D″ anisotropy beneath Africa at the border of the African VLVP, and our observations may help to constrain the northern border of this anomaly. The pattern of shear-wave splitting at DBIC presents an example of the potential pitfalls of using *SKS* splitting to study upper mantle anisotropy. We suggest a set of best practices for measuring and interpreting *SK(K)S*-splitting datasets, which includes examining as much data as possible to maximize back-azimuthal coverage, carefully cataloging null results and interpreting them simultaneously with non-null measurements, and evaluating any discrepancies in *SKS–SKKS* splitting for the same event–station pair. Stations such as DBIC, where the upper mantle beneath the station is apparently isotropic and *SK(K)S* splitting is likely due to lowermost mantle anisotropy, are rare in the global dataset, but careful consideration of back-azimuthal variations, the distribution of nulls, and any *SKS–SKKS*-splitting discrepancies can minimize errors in the interpretation of *SK(K)S*-splitting datasets.

Data and Resources

Data used in this study came from station DBIC of the Global Seismographic Network (GSN) and were obtained from the Data Management Center (DMC) of the Incorporated Research Institutions for Seismology (IRIS). The Splitlab software package (Wüstefeld *et al.*, 2007) was used to measure splitting.

Acknowledgments

We thank the IRIS GSN and DMC programs for making the data available. We are grateful to Martha Savage and an anonymous reviewer for helpful comments. This work was funded by Yale University.

References

Barruol, G., and W. Ben Ismail (2001). Upper mantle anisotropy beneath the African IRIS and Geoscope stations, *Geophys. J. Int.* **146,** 549–561.

Becker, T. W. (2008). Azimuthal seismic anisotropy constrains net rotation of the lithosphere, *Geophys. Res. Lett.* **35,** L05303, doi 10.1029/2007GL032928.

Becker, T. W., S. Lebedev, and M. D. Long (2012). On the relationship between azimuthal anisotropy from shear wave splitting and tomographic models, *J. Geophys. Res.* **117,** no. B01306, doi 10.1029/2011JB008705.

Conrad, C. P., and M. D. Behn (2010). Constraints on lithosphere net rotation and asthenospheric viscosity from global mantle flow models and seismic anisotropy, *Geochem. Geophys. Geosys.* **11,** Q05W05, doi 10.1029/2009GC002970.

Favier, N., and S. Chevrot (2003). Sensitivity kernels for shear wave splitting in transverse isotropic media, *Geophys. J. Int.* **153,** 213–228.

Garnero, E. J., V. Maupin, T. Lay, and M. J. Fouch (2004). Variable azimuthal anisotropy in Earth's lowermost mantle, *Science* **306,** 259–261.

Hanna, J., and M. D. Long (2012). *SKS* splitting beneath Alaska: Regional variability and implications for subduction processes at a slab edge, *Tectonophysics*, doi 10.1016/j.tecto.2012.01.003 (in press).

He, X., and M. D. Long (2011). Lowermost mantle anisotropy beneath the northwestern Pacific: Evidence from *ScS, PcS, SKS,* and *SKKS* phases, *Geochem. Geophys. Geosys.* **12,** Q12012, doi 10.1029/2011GC003779.

Huang, Z., L. Wang, D. Zhao, N. Mi, and M. Xu (2011). Seismic anisotropy and mantle dynamics beneath China, *Earth Planet. Sci. Lett.* **306,** 105–117.

James, D. E., and M. Assumpçao (1996). Tectonic implications of *S*-wave anisotropy beneath SE Brazil, *Geophys. J. Int.* **126,** 1–10.

Kaneshima, S. (1990). Origin of crustal anisotropy: Shear wave splitting studies in Japan, *J. Geophys. Res.* **95,** 11,121–11,133.

Karato, S. (1998). Some remarks on the origin of seismic anisotropy in the D″ layer, *Earth Planets Space* **50,** 1019–1028.

Karato, S., H. Jung, I. Katayama, and P. Skemer (2008). Geodynamic significance of seismic anisotropy of the upper mantle: New insights from laboratory studies, *Annu. Rev. Earth Planet. Sci.* **36,** 59–95.

Karato, S., S. Zhang, and H. Wenk (1995). Superplasticity in the Earth's lower mantle: Evidence from seismic anisotropy and rock physics, *Science* **270,** 458–461.

Kaviani, A., G. Rümpker, M. Weber, and G. Asch (2011). Short-scale variations of shear-wave splitting across the Dead Sea basin: Evidence for the effects of sedimentary fill, *Geophys. Res. Lett.* **38,** L04308, doi 10.1029/2010GL046464.

Kendall, J.-M., and P. G. Silver (1998). Investigating causes of D″ anisotropy, in *The Core-Mantle Boundary Region* M. Gurnis, M. E. Wysession, E. Knittle, and B. A. Buffett (Editors), American Geophysical Union, Washington, D.C., 97–118.

Levin, V., W. Menke, and J. Park (1999). Shear wave splitting in the Appalachians and the Urals: A case for multilayered anisotropy, *J. Geophys. Res.* **104,** 17,975–17,993.

Long, M. D. (2009). Complex anisotropy in D″ beneath the eastern Pacific from *SKS-SKKS* splitting discrepancies, *Earth Planet. Sci. Lett.* **285,** 181–189.

Long, M. D., and T. W. Becker (2010). Mantle dynamics and seismic anisotropy, *Earth Planet. Sci. Lett.* **297,** 341–354.

Long, M. D., and P. G. Silver (2009). Shear wave splitting and mantle anisotropy: Measurements, interpretations, and new directions, *Surv. Geophys.* **30,** 407–461.

Long, M. D., and R. D. van der Hilst (2005). Upper mantle anisotropy beneath Japan from shear wave splitting, *Phys. Earth Planet. In.* **151,** 206–222.

Mainprice, D. (2007). Seismic anisotropy of the deep Earth from a mineral and rock physics perspective, in G. Schubert (Editor), *Treatise on Geophysics*, Vol. **2**, 437–491.

Mattatall, L. R., and M. J. Fouch (2007). Small-scale variations in SKS splitting near Parkfield, California, Fall Meet. Suppl., *Eos Trans. AGU* **88,** Abstract No. T53C-02.

Meade, C., P. G. Silver, and S. Kaneshima (1995). Laboratory and seismological observations of lower mantle isotropy, *Geophys. Res. Lett.* **22,** 1293–1296.

Niu, F., and A. M. Perez (2004). Seismic anisotropy in the lower mantle: A comparison of waveform splitting of *SKS* and *SKKS*, *Geophys. Res. Lett.* **31,** L24612, doi 10.1029/2004GL021196.

Nowacki, A., J. Wookey, and J.-M. Kendall (2011). New advances in using seismic anisotropy, mineral physics and geodynamics to understand deformation in the lowermost mantle, *J. Geodyn.* **52,** 205–228.

Restivo, A., and G. Helffrich (2006). Core-mantle boundary structure investigated using *SKS* and *SKKS* polarization anomalies, *Geophys. J. Int.* **165,** 288–302.

Savage, M. K. (1999). Seismic anisotropy and mantle deformation: What have we learned from shear wave splitting?, *Rev. Geophys.* **37,** 65–106.

Schulte-Pelkum, V., G. Masters, and P. M. Shearer (2001). Upper mantle anisotropy from long-period *P* polarization, *J. Geophys. Res.* **106,** 21,917–21,934.

Silver, P. G. (1996). Seismic anisotropy beneath the continents: Probing the depths of geology, *Annu. Rev. Earth Planet. Sci.* **24,** 385–432.

Silver, P. G., and W. W. Chan (1991). Shear wave splitting and subcontinental mantle deformation, *J. Geophys. Res.* **96,** 16,429–16,454.

Silver, P. G., and M. K. Savage (1994). The interpretation of shear-wave splitting parameters in the presence of two anisotropic layers, *J. Geophys. Res.* **119,** 949–963.

Tian, X., J. Zhang, S. Si, J. Wang, Y. Chen, and Z. Zhang (2011). *SKS* splitting measurements with horizontal component misalignment, *Geophys. J. Int.* **185,** 329–340.

Vanacore, E., and F. Niu (2011). Characterization of the D″ layer beneath the Galapagos Islands using *SKKS* and *SKS* waveforms, *Earthq. Science* **24,** 87–99.

Vecsey, L., J. Plomerova, and V. Babuska (2008). Shear-wave splitting measurements—Problems and solutions, *Tectonophysics* **462,** 178–196.

Wang, Y., and L. Wen (2007). Complex seismic anisotropy at the border of a very low velocity province at the base of the Earth's mantle, *J. Geophys. Res.* **112,** no. B09305, doi 10.1029/2006JB004719.

Wirth, E., and M. D. Long (2010). Frequency-dependent shear wave splitting beneath the Japan and Izu-Bonin subduction zones, *Phys. Earth Planet. Int.* **181,** 141–154.

Wookey, J., and J. M. Kendall (2007). Seismic anisotropy of post-perovskite and the lowermost mantle, in *Post-Perovskite: The Last Mantle Phase Transition*, K. Hirose, J. Brodholt, T. Lay, and D. Yuen (Editors), American Geophysical Union, Washington, D.C., 171–189.

Wüstefeld, A., G. H. R. Bokelmann, G. Barruol, and J. P. Montagner (2009). Identifying global seismic anisotropy patterns by correlating shear-wave splitting and surface-wave data, *Phys. Earth Planet. In.* **176,** 198–212.

Wüstefeld, A., G. Bokelmann, G. Barruol, and C. Zaroli (2007). Splitlab: A shear-wave splitting environment in MATLAB, *Comp. Geosci.* **34,** 515–528.

Department of Geology and Geophysics
Yale University
P.O. Box 208109
New Haven, Connecticut 06520
colton.lynner@yale.edu

Manuscript received 12 September 2011